RESEARCH ARTICLE

OPEN ACCESS

Deep Learning Based Ovarian Cancer Classification Using EfficientNetB2 with Attention Mechanism

Jayashri Kolekar¹, Chhaya Pawar², Amol P Pande¹, and Chandrashekhar M Raut¹

- ¹ Computer Engineering Department, Datta Meghe College of Engineering, Navi Mumbai, India
- ² Computer Engineering Department, Agnel Charities' Fr. C. Rodrigues Institute of Technology, Navi Mumbai, India

Corresponding author: Jayashri Kolekar. (e-mail: jayashriphonde@gmail.com), **Author(s) Email**: Chhaya Pawar (e-mail: chhaya.pawar@fcrit.ac.in, Amol P Pande (e-mail: amol.pande@dmce.ac.in), Chandrashekhar M Raut (e-mail: chandrashekhar.raut@dmce.ac.in)

Abstract Ovarian cancer is a gynecological malignancy comprising multiple histopathological subtypes. Traditional diagnostic tools like histopathology and CA-125 tests suffer from limitations, including interobserver variability, low specificity, and time-consuming procedures, often leading to delayed or incorrect diagnoses, which are subjective and error-prone. Conventional machine learning models, such as K-Nearest Neighbors (KNN) and Support Vector Machine (SVM), have been applied but often struggle with high-dimensional image data and fail to extract deep morphological features. This study proposes a DLbased framework to classify ovarian cancer subtypes from histopathological images, aiming to enhance diagnostic accuracy and clinical decision-making. Initially, Deep learning was applied using pre-trained architectures such as VGG-16, Xception, and EfficientNetB2. However, the standout innovation in this study is the integration of EfficientNetB2 with Convolutional Block Attention Module (CBAM), an attention mechanism module. An attention mechanism allows the model to focus on the most informative regions of the image, thereby improving diagnostic precision. The proposed system was trained and validated on a diverse, well-structured dataset, achieving high accuracy and strong generalization capability. EfficientNetB2 with CBAM outperformed other models, achieving a 91% accuracy rate compared to 52% for VGG-16, 72% for Xception, and 82% for the baseline EfficientNetB2 model. This attention-enhanced, scalable AI model demonstrates strong potential for clinical application. It provides faster and more efficient classification of ovarian cancer subtypes compared to conventional approaches. The framework has the potential to improve survival outcomes for patients with ovarian cancer. The proposed system demonstrates a significant improvement in ovarian cancer subtype classification (High-Grade Serous Carcinoma, Low-Grade Serous Carcinoma, Clear-Cell, Endometrioid, and Mucinous Carcinoma). It provides a practical tool for aiding early diagnosis and treatment planning, with potential for integration into clinical workflows.

Keywords Ovarian Cancer, Cancer Subtype Classification, Histopathological Image Analysis, Deep Learning, EfficientNetB2.

I. Introduction

Ovarian cancer is a deadly gynecological cancer sometimes labeled as the "silent malignancy" due to its asymptomatic nature in the initial stages and the lack of effective screening tests [1]. The disease is not monolithic; it comprises several distinct histological subtypes, each characterized by unique genetic and molecular profiles, clinical behavior, and responses to therapy. These subtypes include High-Grade Serous Carcinoma (HGSC), Clear-Cell Ovarian Carcinoma (CC), Endometrioid (EC), Low-Grade Serous Carcinoma (LGSC), and Mucinous Carcinoma (MC) [2]. Accurate classification of these subtypes is crucial

because treatment strategies and prognoses vary significantly among them. Traditional diagnostic methods, such as CA-125 blood tests and ultrasound imaging, often lack specificity and fail to accurately distinguish between benign and malignant tumors [3]. Women who are in their forties and above are most commonly diagnosed with ovarian cancer, even though it can occur at any age. The disease typically goes undetected until it has spread within the pelvis and abdomen, making early diagnosis challenging and reducing the chances of effective treatment [4]. Due to the lack of reliable screening methods, there is a growing need for advanced computational tools to

support early and accurate diagnosis [5]. Recent advancements in artificial intelligence and DL offer promising approaches to classify ovarian cancer subtypes based on medical, pathology slides, or molecular data, potentially improving patient outcomes through personalized treatment strategies.

However, many conventional machine learning models have shown limited success due to their inability to handle high-dimensional image data and extract complex morphological features from histopathological slides [6]. While deep learning (DL) has emerged as a powerful alternative, there remains a need to optimize an architecture that can not only achieve high accuracy but also provide explainable and robust predictions suitable for clinical use.

To address these limitations, this study proposes a novel architecture combining EfficientNetB2 with CBAM. The integration of the CBAM attention wrapper allows the model to focus selectively on the most informative spatial and channel features in medical images, thereby improving diagnostic accuracy. This model outperformed other baseline and state-of-the-art DL architectures in our experiments, achieving a classification accuracy of 91% on five ovarian cancer subtypes. Additionally, a Flask-based graphical user interface (GUI) was developed to enhance clinical usability. This work not only bridges the gap between diagnostic accuracy and practical deployment but also sets a benchmark for future research in ovarian cancer subtype classification using attention-based DL models. The major contributions of this study include the development of a hybrid EfficientNetB2-CBAM architecture that integrates spatial and channel attention for improved feature extraction, achieving 91% accuracy across five ovarian cancer subtypes. Additionally, it creates a Flask-based GUI to enhance clinical usability and enable real-time application.

This study is structured as follows: Section II reviews related works and recent advances in ovarian cancer detection and classification. Section III discusses the proposed workflow, the dataset used, the dataset preprocessing, and the methodology. Section IV displays the experimental results of DL models and performance evaluation. Section V discusses the interpretation and comparison of results with other studies and limitations. Section VI, conclusions, which rewrite the objectives, main findings, and future works.

II. Related Works

Effective prediction and accurate classification of ovarian cancer are critical for timely diagnosis and treatment [7]. Existing research can be broadly categorized into two main areas: ovarian cancer detection and classification. This section provides a detailed review of prior work in both areas. Table 1 highlights recent studies on ovarian cancer detection

using DL and ML. Table 2 focuses on studies performing ovarian cancer subtype classification using DL. The reviewed study highlights their approaches, limitations, strengths, and the achieved accuracies. From these works, it is evident that no study to date has leveraged EfficientNetB2 architectures with CBAM for subtype classification, and accuracy has typically topped out around 84% in prior efforts. This motivates our proposed approach to further enhance performance.

A. Ovarian Cancer Detection

The study proposed in [8] utilizes ML techniques to classify ovarian cancer based on clinical data. The aim was to enhance early diagnosis, which is challenging due to the absence of distinctive symptoms even at later stages. The study utilized data with 203 instances. Working with a limited size of dataset was one of the challenges in the study, which may affect the generalization of the model. With these challenges, however, this study demonstrated that both KNN & SVM are effective in classifying ovarian cancer, albeit the small dataset may not permit robustness and application of the model in large and diverse populations.

The work presented in [9] suggests an approach to predicting the survival of ovarian cancer patients based on machine learning. The objectives of the study were to design both classification and regression models for the purpose of predicting patient survival with the help of six ML techniques. The SHAP method was applied to explain the decision-making process and determine the most influential aspects that affect survival predictions. According to the study, RF was the best for classification while XGBoost was best for regression (RMSE = 20.61%, R² = 0.4667). Some of the most significant features influencing survival predictions included histologic type. The main challenge faced in the study was the complexity of integrating multiple machine learning models with interpretability methods, which required balancing model performance with clarity. Despite the high accuracy and robustness of the models, the approach could be limited by the need for large, high-quality datasets to maintain its effectiveness and generalizability. Additionally, while the SHAP method improved model transparency, it may still require expert interpretation for complex cases. Nonetheless, this study is significant as it is the first to apply multiple ML models for ovarian cancer survival prediction using the SEER dataset and incorporates SHAP to enhance model transparency for clinical use.

In [10], the authors suggested an AI approach to ovarian endometriomas (OEs) that tend to be misdiagnosed because of their symptoms' resemblance to the common gynecological emergencies. The work initiates a particle swarm optimization (PSO). There is one challenge that has

Table 1. Overview of Existing Research on Ovarian Cancer Detection

Study	Contribution	Method	Results	Limitations	Future Direction
[8]	Early diagnosis of ovarian cancer using ML on clinical records	KNN, SVM	KNN: 90.47% Accuracy, 94.11% F1-score; SVM: 90.47% Accuracy, 92.30% F1-score	Small dataset size (203 instances) limits generalizability	Expand dataset size; test on diverse populations to improve robustness
[9]	Predict survival of ovarian cancer patients with explainable ML	KNN, SVM, DT, RF, AdaBoost, XGBoost + SHAP for interpretability	RF (Classification): 88.72% Accuracy, 82.38% AUC; XGBoost (Regression): RMSE = 20.61%, R ² = 0.4667	Complex integration of models and interpretability tools; SHAP requires expert analysis	Enhance clinical integration; explore deep learning with interpretability for better performance.
[10]	Al-enabled early diagnosis of ruptured ovarian endometriomas (OEs)	Particle Swarm Optimization enhanced Random Forest (PSO-RF)	Accuracy: 97.47%, AUC: 0.996, Sensitivity: 94.12%, Specificity: 98.39%	Performance may vary on small/diverse datasets; the fairness of the model comparison	Test model on diverse, multi- center datasets to assess generalizability
[11]	Efficient prediction of ovarian cancer using reduced features	RF model with PCA, K-PCA, and ICA for dimension reduction	Best with PCA: F1 Score: 0.895, Training time: 18.191s	Limited to one dataset; no comparison with other ML models	Evaluate on different datasets; compare with alternative classifiers
[12]	Ultrasound- based tumor classification with image enhancement	CNN integrated with Convolutional Autoencoder (CAE) using DenseNet121/161	Accuracy: 97.2%, AUC: 0.9936 (normal vs tumor), 90.12% (malignant classification)	Limited generalizability due to dataset size and diversity	Test with larger, multi-source datasets; clinical validation
[14]	ROI-based image classification for better ovarian cancer detection	Region-based CNN with SVC and Gaussian NB ensemble	Precision: >95%, SVC: 95.96%, NB: 97.7%; Specificity: up to 98.69%	Relies on manual annotations; needs testing on diverse images	Automate annotations; expand testing across clinical settings
[15]	CT image-based classification using hybrid deep learning	Xception + Vision Transformer (ViT) + MLP	Accuracy: 98.09% (OCCTD), 96.05% (BOTD), 98.73% (MOTD)	Depends on dataset quality/diversity; may not generalize across populations	Validate with broader datasets and other imaging modalities

been faced in this study was securing the fairness of comparisons, as all models were optimized using the same parameter-tuning techniques. While the results are promising and the approach may face limitations when applied to smaller or larger datasets, as the model's performance could change with data quality and the generalizability of the training data.

The proposed model by [11] is an RF-based ovarian cancer prediction model, which is designed to predict the presence of ovarian cancer using a dataset with some features. Given that a dataset with high dimensionality can increase the time and resources

required for model training, the study applied dimension reduction techniques to reduce the dimensionality of the data and assess their impact on both prediction accuracy and computational performance. The best results were obtained with PCA, which reduced the size of the data from 49 features to 6, with an F1 score of 0.895, and the time of training the model was cut down to 18.191 seconds. Not only did this approach led to a more precise prediction, but it turned out to be more cost and time efficient, in comparison to the use of a full dataset without any dimension reduction. The study emphasizes the advantages of using dimension reduction methods for

analyzing large-scale medical data, as both the accuracy of the prediction results and resource utilization can benefit from this approach. Nevertheless, the weakness of the approach is that it is based on a fixed dataset, and the model's performance may change for other datasets featuring different distributions of features or their quality. Furthermore, the study did not examine other machine learning models that could provide additional performance improvements through their implementation.

The work in [12] suggested the creation of a CNN-CAE model of CNN incorporating a convolutional autoencoder for detecting ovarian tumors from ultrasound images. The employed dataset included 1613 ultrasound images of ovaries that were clinically diagnosed, which were pre-processed and augmented in order to run deep learning-based analysis. The CNN-CAE model was developed to get rid of the unwanted information, like calipers, and categorize the ovaries into five classes. The performance of the model was measured using fivefold cross-validation; accuracy. sensitivity, specificity, and the AUC were some of the metrics used to analyze the model. The CNN-CAE model performed well, and its performance was 97.2% accuracy, 97.2% sensitivity, and an AUC of 0.9936 in determining the normal versus the ovarian tumors with an architecture of DenseNet121. To discriminate malignant ovarian tumors, an accuracy of 90.12%, a sensitivity of 86.67%, and an AUC of 0.9406 were attained by the model using the DenseNet 161 architecture. In addition, Grad-CAM was used to observe the model's decision-making process [13], and it appeared that in the ultrasound image, the model identified significant texture and morphological aspects. Although the study reveals that the CNN-CAE model is an efficient and viable tool for predicting ovarian tumor classification, a weakness is identified regarding the influence of the quality and range of ultrasound images in the training set on the model's generalizability. Additional testing on varied and larger datasets may enhance the model's utility in clinical work.

In [14], the authors introduced a new scheme for ovarian cancer classification based on a rapid region-based network, where emphasis is laid upon the region of interest (ROI) segmentation of the ovarian images. The study was conducted with the attempt to increase the classification accuracy for the purpose of better decisions for the treatment, because there is a need for early and accurate diagnosis to decrease mortality rates. The input ovarian images were classified into three types of cells. Epithelial, germ, and stroma cells that were segmented and pre-processed before the FaRe-ConvNN model was used for annotations. The model used the region-based classification for comparison with manually annotated features and

trained ones by FaRe-ConvNN. The study employs a combined method of Support Vector Classification (SVC) and Gaussian Naive Bayes (Gaussian NB) classifiers to produce the classification after the regionbased training is complete. Ensemble method was applied in the process of feature classification, enhancing indexing of the data and data classification. The results revealed that FaRe-ConvNN achieved a precision of more than 95%, whereas SVC and Gaussian NB obtained 95.96% and 97.7% precision, respectively. Sources for the recall were 94.31% for SVC and 97.7% for Gaussian NB, while specificity was recorded at 97.39% and 98.69% for SVC and Gaussian NB, respectively. FaRe-ConvNN improved precision in Gaussian NB. Although the method showed high accuracy and perspectives of the enhanced diagnosis, a shortcoming is that this system depends on the quality of visual annotations that might introduce errors, and it might have to be checked on other datasets or real-life situations.

The proposed study [15] presented a hybrid Xception_ViT model for the detection and classification of ovarian cancer based on computed tomography (CT) images. The objective of the given study was to make the diagnostic process of ovarian cancer more accurate and effective, which is still a significant problem, because of high mortality rates and the absence of an exact diagnostic method. The results imply that the proposed model can clearly divide ovarian tumors and can significantly help inexperienced radiologists and gynecologists in making a diagnosis of ovarian malignancies and offering alternative decision tree preferences. However, one limitation of the method may be its dependence on the quality and variety of the CT datasets, as well as its generalizability to other populations and imaging modalities.

B. Ovarian Cancer Classification

The proposed system in [16] used a DCNN based on AlexNet to identify types of ovarian cancer within cytological images [17]. The augmented images, together with the original images, were used to train the model, which achieved an enhanced classification accuracy of 78.20% compared to 72.76%. The study encountered two major limitations, including reduced dataset quantity together with the risk of overfitting.

In [18], the proposed system evaluated ML-based image classification models that would support pathologists in diagnosing ovarian carcinoma histotypes through training four DCNNs using WSIs dyed with hematoxylin and eosin (H&E). The model's optimal performance is demonstrated by more than 80% agreement in both training situations and independent external data, while providing descriptions that prove better than those of human expert pathologists. The positive outcomes from research

Table 2. Overview of Existing Research on Ovarian Cancer Classificati

Study	Contribution	Method	Accuracy	Limitations	Future Direction
[16]	Classification of ovarian cancer subtypes based on cytological images	DCNN based on AlexNet	78.20%	Small dataset and overfitting	Test model on diverse, multi-center datasets to assess generalizability
[18]	Improve pathologists' agreement on ovarian carcinoma histotypes	DCNN models for histopathological slide classification	81.38%	Requires validation across multiple institutions	Test with larger, multi- source datasets
[19]	Prediction and categorizing ovarian cancer subtypes	Modified AlexNet-based DCNN	83.93%	High computational complexity	Use of different DL model to improve accuracy
[20]	Classify ovarian epithelial carcinoma into four subtypes	VGG-16 models for histopathological slide classification	84%	Accuracy leaves room for improvement	DCNN enhancement, User interface development

should be supported by the expanded use of extensive datasets across multiple medical facilities for validation purposes.

According to [19], a new Deep Convolutional Neural Network (DCNN) structure was introduced, which is designed to to recognize and categorize different ovarian cancer subtypes using histopathological images. CT and MRI represent traditional diagnostic tools, but they prove expensive because they demand lengthy processing, and an efficient replacement is needed. Full implementation of this model, adapted from AlexNet, involved adding one more maxpooling layer after two convolutional layers (resulting in four total iterations). It also involved creating four fully connected layers and replacing the (Rectified Linear Unit) ReLU activation function by Exponential Linear Unit (ELU) and normalizing all kernel sizes to 3×3. With 24,742 augmented images used for training, the model achieved an accuracy of 83.93%, thereby surpassing prior achievements based on an accuracy of 78%. The study establishes that performance enhancement was possible through the application of augmentation techniques. The high number of parameters at 43, 94, 533 might affect real-time system processing speed due to increased computational complexity.

In [20], the proposed system uses VGG-16 as a pretrained DCNN model for classifying ovarian cancer subtypes through histopathological images is demonstrated in the proposed system. The model began with 500 images during training and achieved 50% accuracy before being enhanced to 84% through dataset augmentation, after processing 24,742 images. Deep learning methods proved effective in medical diagnosis tasks for ovarian cancer. Still, data restrictions coupled with model memorization behaviors along with image quality sensitivities, acted as continuing barriers to progress.

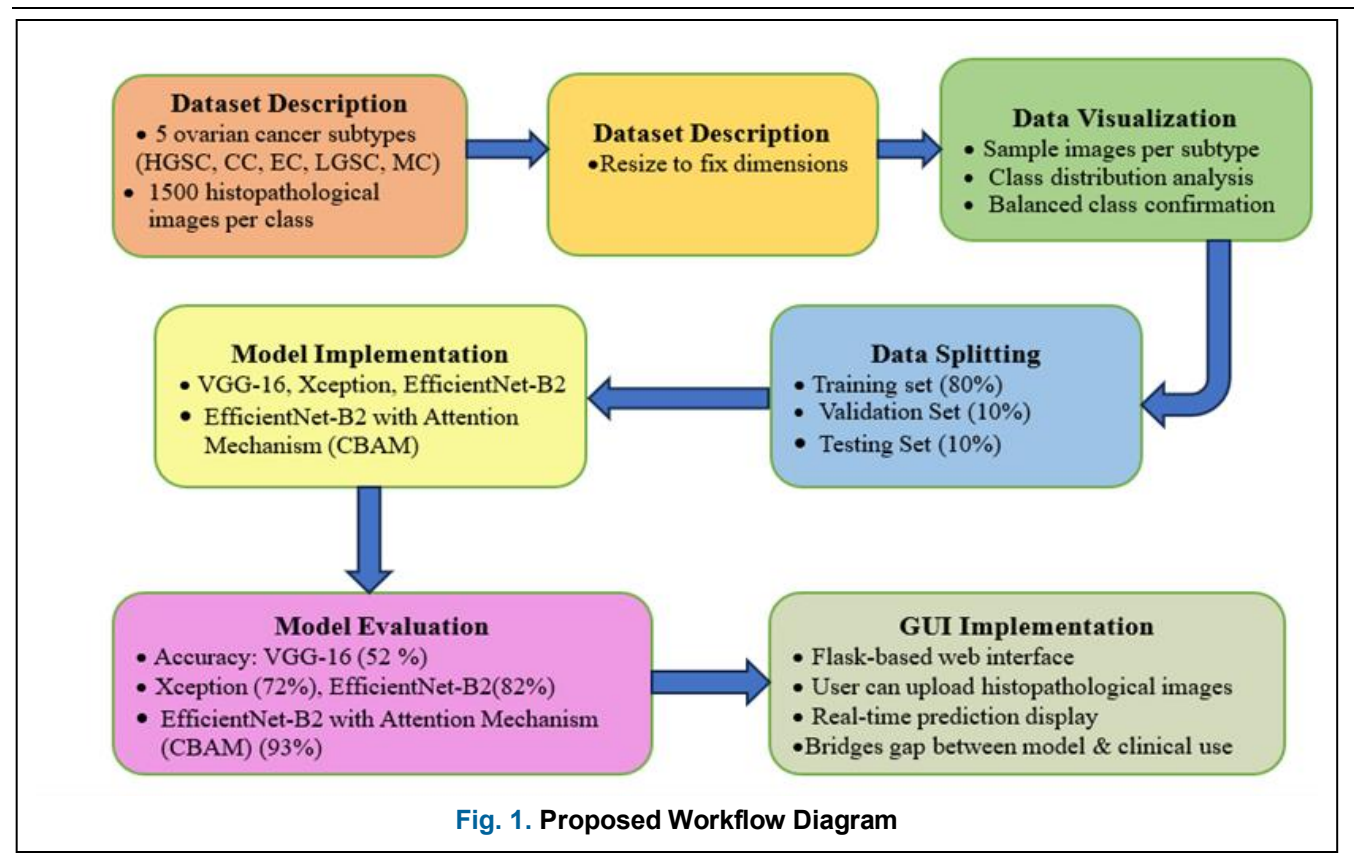
III. Method

A. Proposed Workflow

The proposed workflow shown in the Fig. 1. acquisition encompasses the and meticulous preprocessing of medical imaging data, followed by the training of advanced deep learning architectures, VGG-16, Xception, dan EfficientNetB2 selected for their advanced feature learning capabilities. The dense layers of these models are fine-tuned to classify ovarian cancer subtypes. Lastly, EfficientNetB2 is combined with transfer learning and a channel attention mechanism (CBAM) to refine feature extraction and enhance classification accuracy. The performance of each model is rigorously evaluated using pivotal metrics. This strategic approach optimizes performance while ensuring efficient and accurate subtype classification.

B. Dataset Description

The dataset used for this research is sourced from [21] and discussed in the context of ovarian cancer subtypes classification based on histopathological image data. The dataset contains images, representing five major subtypes of epithelial ovarian cancer (HGSC, CC, EC, LGSC, and MC). Each of these subtypes has unique histopathological features, molecular profiles, and clinical representations, and thus an accurate classification is necessary to ensure the formulation of effective and personalized treatment strategies. Currently, manual histological assessment remains the



primary method for subtype identification, although it can be laborious and subjective. It is through the use of data science and DL that the ability lies to improve the accuracy and speed of diagnostics, in assisting clinicians to make more informed decisions.

The dataset was curated with care in order to promote this goal while ensuring adequate representation of the five major subtypes. A balanced subset of 1500 images per class was used for this project, with regard to limitations of computational resources and availability of GPU. Such a technique enables consistency in training at the same time avoiding biases towards a particular class. The dataset therefore creates a strong basis for training and testing of the DL models and potential automatic subtype determination of the ovarian cancer. Through image analysis techniques and neural networks, this research aims the purpose of enhancing the prediction of subtypes contributing to the progress of precision oncology.

C. Data Processing

During the data preprocessing phase, several key steps were taken to prepare the dataset for training the ovarian cancer image model. Along with image resizing, categorical labeling of the data was performed as an additional preprocessing step. Given that the set of data contains five different subtypes of ovarian cancer, each subtype was assigned a certain label. These tags were further encoded into a numerical format prepared for

multiclass classification. This ensures that the models interpret the output classes correctly during training. These preprocessing methods help normalize the dataset, remove bias, and improve the model's performance. Besides, attention was paid to the processing of missing or unreadable images to avoid training errors. On the whole, the preprocessing pipeline played a central role in organizing the data and labels of

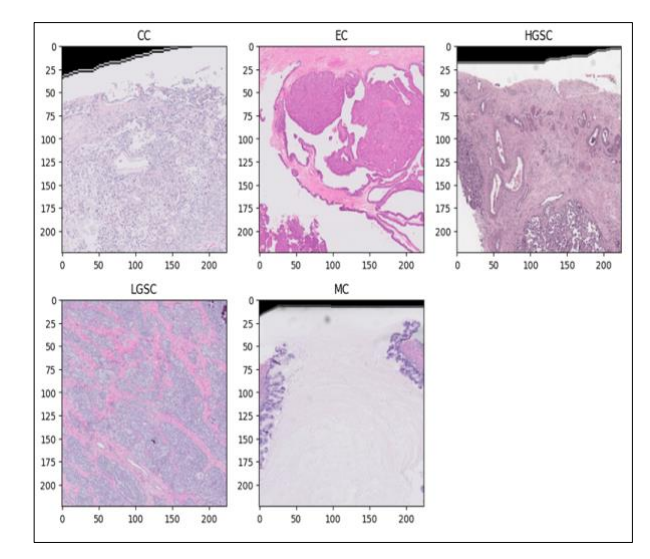


Fig. 2. Sample Images from Each Ovarian Cancer Subtype

the images so that they were in a consistent, machinereadable format, which provided a solid setup for the accurate and effective classification of those by the deep learning models.

D. Data Visualisation

Fig. 2. illustrates representative sample images from the five ovarian cancer subtypes included in the dataset. These images were visualized as part of the Exploratory Data Analysis (EDA) phase to gain initial insights into the morphological patterns and differences among the subtypes. Each image represents a histopathological slide captured under a microscope, with variations in cell structure, tissue density, and staining intensity clearly visible. For instance, the CC image displays prominent cell nuclei with dense clustering, while HGSC exhibits complex glandular patterns with darker staining. EC and LGSC demonstrate relatively structured tissue formations. whereas MC shows loosely organized tissue with lighter staining. This visual inspection not only confirms the presence of distinct cellular features among subtypes but also highlights the challenges in classification due to overlapping characteristics in certain cases. EDA like this is vital for understanding the dataset before modeling, as it helps in detecting any anomalies, understanding class distributions, and validating the diversity and quality of image data. These insights guide model selection and preprocessing strategies, ensuring the deep learning model is wellinformed and robust.

A count plot in Fig. 3. shows the distribution of image samples across the five ovarian cancer subtypes. The plot confirms that the dataset is well-balanced, with approximately 1500 image samples allocated to each class. This uniform distribution is a crucial aspect of data integrity, as it prevents class imbalance during model training a common issue in medical image classification that can lead to biased predictions and reduced generalizability.

E. Data Splitting

For model training and evaluation, the dataset was divided into three subsets: training, validation, and testing, using an 80:10:10 ratio. This means 80% of the data was allocated for training the DL models, allowing them to learn patterns and features relevant to classifying ovarian cancer subtypes. Ten percent was set aside for validation, enabling fine-tuning of model parameters and monitoring performance during training to prevent overfitting. The remaining 10% was reserved for final testing, providing an unbiased evaluation of the model's generalization ability. This split ensures a balanced and systematic approach to model development and assessment. With the dataset preprocessed and split into training, validation, and testing sets, several deep learning models were finetuned, as described in the following subsection.

F. Model Architecture and Training

The experiments employed three DL architectures: VGG16, Xception, and EfficientNetB2, a baseline model, and an enhanced model with CBAM. VGG-16, known for its depth and simplicity, and useful as a baseline. The Xception model stands out as an innovative iteration among convolutional neural networks, showcasing its superiority with advanced architectural layers that excel in image classification tasks. EfficientNetB2 is part of the EfficientNet family, which stands out for its use of a compound scaling method that uniformly scales all dimensions of the



Fig. 3. Class Distribution of Ovarian Cancer Subtypes

model's architecture depth, width, and resolution. This coherent scaling results in a highly efficient model that achieves superior performance with fewer parameters and reduced computational costs. To further improve the feature extraction and improve the accuracy of classification of ovarian cancer, the CBAM, an attention mechanism module integrated with EfficientNetB2.

G. EfficientNetB2 with CBAM

The integration of EfficientNetB2 with an attention mechanism and transfer learning serves as the pinnacle of our model development strategy, aiming for optimal efficiency and classification performance. To enhance feature extraction, the CBAM module is incorporated with EfficientNetB2. The channel attention in CBAM identifies which feature maps (filters) are most important by aggregating spatial information, and spatial attention then finds where in the image the important features are, by looking at all channels.

In the proposed system, Fig. 4. shows the EfficientNetB2 base architecture [22], initially trained on the ImageNet dataset, which provides a robust backbone for feature extraction. By utilizing transfer learning, the early layers of EfficientNetB2 were frozen, and the top layers were fine-tuned, inserting the CBAM module before the final classification layer to effectively

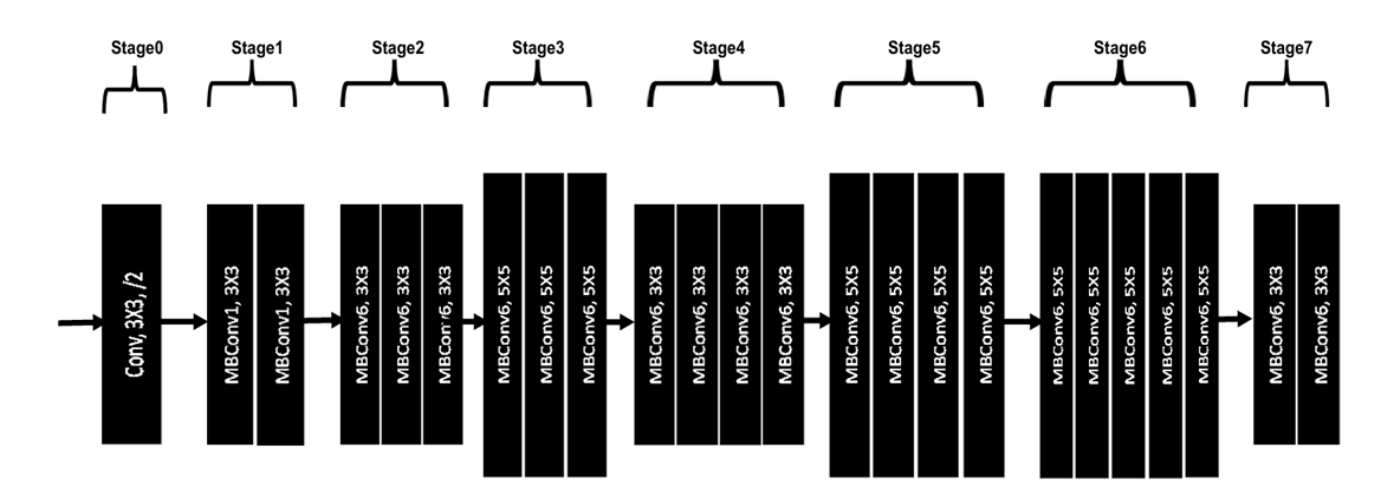


Fig. 4. EfficientNetB2 Architecture [22]

harness its comprehensive understanding of image features, dramatically accelerating the training process specific to our ovarian cancer dataset. This pre-training equips the model with a finely tuned ability to identify complex patterns within histopathological images related to different ovarian cancer subtypes, including HGSC, CC, EC, LGSC, and MC.

To further enhance the feature extraction capability of EfficientNetB2, an attention mechanism is incorporated. This mechanism strategically refocuses the network's attention onto the most relevant areas of an image, elevating its sensitivity to subtle differences across cancer subtypes. Attention mechanisms work by weighing feature maps, allowing the network to prioritize significant features while filtering out noise, thus improving accuracy in differentiating subtypes.

The model begins with the input layer, which accepts an image with a standard size of 224 x 224 [23]. It is followed by the regular convolutional layers with 3x3 filters [23], which is also called the stem layer, making up the first layer, the convolution operation is evaluated using Eq. (1)

$$X_c(i,j,k) = \sum_m \sum_n \sum_c X(s.i+m,s.j+n,c)$$
. $K(m,n,c,k)$ (1) where X is the input tensor, K is the filters, s is the stride, c is the channel depth, and k is the output channel index [24]. Then, apply the batch normalization to normalize the convolution output, and the Swish activation function Eq. (2) is applied to reduce the spatial resolution.

$$Swish(x) = x \frac{1}{1 + e^{-x}} \tag{2}$$

This activation is used throughout EfficientNet instead of ReLU because it empirically improves accuracy with minimal computational overhead. The output is given as input to the Mobile Inverted Bottleneck Convolution (MBConv) block. The MBConv block is a specialized

building block designed for efficient computation and high accuracy. Each MBConv block includes an expansion Phase, which applies a pointwise 1X1 convolution Eq. (3) to increase the number of channels by a factor t.

$$X_{exp}(i,j,k) = \sum_{c} X(i,j,k) . K_{exp}(c,k)$$
 (3)

where $X_{exp}(i,j,k)$ is the expanded tensor. Then the depthwise convolution Eq. (4) is applied independently to each channel using (3X3 or 5X5) kernel, to extract spatial features per channel efficiently.

$$X_{dw}^{k} = X_{exp}^{k} * k_{dw}^{k}$$
 for $k = 1,...,t C_{in}$ (4)

After this, the Squeeze and Excitation (SE) block, which globally squeezes each channel to a scalar, learn important weights and rescales. It begins with Eq. (5) global average pooling to squeeze spatial dimensions

$$Z_k = \frac{1}{H.W} \sum_{i=1}^{H} \sum_{j=1}^{W} X_{dw}(i,j,k)$$
 for $k = 1,...,t$ C_{in} (5)

These values pass through two fully connected layers with a ReLU and sigmoid activation to generate channel-wise weights, and SE is scaled by Eq. (6), and the output becomes

$$X_{se}(i, j, k) = X_{dw}(i, j, k). s_k$$
 (6)

Next, a projection layer reduces the expanded channels back using another pointwise convolution and residual connection with Eq. (7) and Eq. (8) to add input to output.

$$X_{proj}(i,j,k) = \sum_{c} X_{se}(i,j,c) . K_{proj}(c,k)$$
 (7)

$$Y(i,j,k) = X_{in}(i,j,k) + X_{proj}(i,j,k)$$
(8)

These MBConv block is repeated in various stages of EfficientNetB2, with different numbers of filters and strides. The SE, which is a part of the MBConv block, only concentrates on the channel-wise features, so to enhance the feature extraction and retrieve the spatial attention features also a CBAM module is introduced

after the final MBConv block. CBAM sequentially applies both channel and spatial attention, allowing the network to focus not only on the most informative feature maps but also on the most relevant spatial regions [25]. The CBAM module progressively applies channel and spatial attention. Channel attention generates feature map global descriptors using global average and max pooling. These pooled descriptors are communicated across fully shared linked layers and sigmoid (σ) modified to blend and activate their outputs to normalize channel weights.

 $Fc = \sigma(MLP(AvgPool(Y(i, j, k))) + MLP(MaxPool(Y(i, j, k))))(9)$ [26]

Classification-relevant channels are improved by multiplying these weights from Eq. (9) on the feature maps. Each feature map's spatial attention mechanism detects key spatial regions. Two 2D maps of average and maximum activations result from channel-wide pooling. Concatenating and convolving these maps with a small kernel captures spatial dependencies.

$$Fs = \sigma(Conv(AvgPool(Y'(i, j, k))). (MaxPool(Y'(i, j, k))))$$
(10) [26]

The element-wise spatial attention weights of the sigmoid function are applied to channel-refined feature maps. A sequential attention design allows the model to prioritize global channel-level importance and then fine-tune attention to local spatial regions, improving interpretability and histopathology slide representation of diagnostically significant places. The Channel-wise feature extraction is done with Eq. (11)

$$Y_c(i,j,k) = M_c(k) + Y(i,j,k)$$
(11)

And the spatial attention features are extracted with Eq. (12)

$$Y(i,j,k) = M_s(i,j) + Y_c(i,j,k)$$
 (12)

At the final stage, global average pooling is applied.

$$Z_k = \frac{1}{HW} \sum_{i=1}^{H} \sum_{j=1}^{W} Y(i,j,k)$$
 (13)

Eq. (13) generates a feature vector that is passed through a fully connected dense layer with SoftMax activation, Eq. (14), to produce the class probabilities for the subtype classification.

$$P(\hat{\mathbf{y}}k) = \frac{e^{z_K}}{\sum_{j=1}^{C} e^{z_j}}$$
 (14)

$$\mathcal{L} = -\sum_{k} y_{k} \cdot \log \hat{y}_{k} \tag{15}$$

The loss function, a categorical cross-entropy equation (Eq. 15), is used to compare predictions with true labels. The model weights are updated using the Adam optimizer with a learning rate of 0.0001 [27] [28]. Each of these steps contributes to training an effective model for classifying ovarian cancer subtypes, leveraging pretrained knowledge from EfficientNetB2 enhancing critical features through attention mechanisms.

This dual approach, which leverages EfficientNetB2's pre-training and attention

mechanisms, leads to a more refined model that operates with improved classification precision and reliability. By enhancing the model's ability to focus selectively on critical regions of the input images, we're better equipped to support accurate diagnosis and facilitate informed clinical decisions. As a result, this implementation suggests significant advancements in the realm of automated cancer classification. Throughout the training phase, an iterative process of hyperparameter tuning was conducted to optimize the performance of each model. Key parameters, such as learning rates and batch sizes, were delicately chosen and refined, ensuring that the models were not only accurate but also efficient in processing data. The convergence of models was regularly evaluated to ensure reliable performance in classifying the five major subtypes of ovarian cancer.

Following the training phase, the model underwent a rigorous validation process to ensure its reliability and effectiveness. During validation, the model's predictions were compared against the true labels. allowing us to gauge its performance on new data and identify potential overfitting. Key metrics, such as accuracy and loss, were closely monitored to understand the model's learning curve and overall effectiveness. lf а model underperforms, hyperparameters are fine-tuned or adjusted the architecture followed by retraining. This iterative validation process ensures that the models are robust and capable of accurately classifying ovarian cancer subtypes in clinical settings.

H. Mathematical Formalization of EfficientNetB2 with CBAM

EfficientNetB2–CBAM processes features, refines attention, and classifies. A feature extraction backbone convolutional block learns hierarchical feature representations from an input image by convolution, normalization, and activation. This can be expressed as Eq. (16) [29]:

$$F_l = \delta \big(BN(W_l * F_{l-1} + b_l) \big) \tag{16}$$

Where, F_{l-1} is the input tensor, W_l and b_l denotes weights and bias, * is the convolution operation and δ is the Swish activation function, denoted by Eq. (1)

Each block's intermediate output F_i gives the attention module spatially encoded semantic patterns. The Convolutional Block Attention Module enhances these qualities by sequentially applying channel and spatial attention, as outlined in Eq. (9) to Eq. (12). Channel attention weights feature maps, thereby boosting relevant channels and reducing duplicates. Spatial attention localizes important regions in feature maps using pixel-wise significance weights from global pooling. Classifiers receive revised tensors F_s with selectively emphasized characteristics in process. average Global pooling compresses spatial

dimensions into a compact vector representation using Eq. (13).

The feature vector $Z = [Z_1, Z_2, \dots, Z_C]$ is then passed to a fully connected layer with a SoftMax activation function classifies. The five ovarian cancer subtypes' probability distribution is derived from the feature vector. EfficientNetB2's global context awareness and CBAM's local discriminative capacity improve pipeline sensitivity to subtype-specific histopathological Variations in Process.

I. Formalizing and Optimizing Loss Function

A categorical cross-entropy guides learning by comparing class labels to expected probability distributions. The model predicts a vector of probabilities for all subtypes in each picture sample $P_i = [P_{i1}, P_{i2}, \dots, P_{iK}]$, while the corresponding true label is encoded as a one-hot vector $y_i = [y_{i1}, y_{i2}, \dots, y_{iK}]$

The loss for each sample is calculated with Eq. (15), which is the negative logarithm of the right class probability.

$$\mathcal{L}_{total} = \frac{1}{N} \sum_{i=1}^{N} \sum_{k=1}^{C} y_k^i \log \hat{y}_k^i$$
 (17) [30]

As expressed in Eq. (17) total loss function, the optimization target, is calculated from all samples. The Adam technique optimizes parameter learning rates using first- and second-order gradient estimations with Eq. (18) and Eq. (19) as follows [31]:

$$m_t = \beta_1 m_{t-1} + (1 - \beta_1) g_t \tag{18}$$

$$v_t = \beta_2 v_{t-1} + (1 - \beta_2) g_t^2$$
 (19)

Where β_1 and β_2 are decay rates and g_t is the gradient of the loss function.

The momentum and decay terms of Adam smooth convergence and prevent parameter update oscillations. To avoid overfitting and numerical instability, the learning rate, starting at 0.0001, is dynamically scaled down whenever the validation accuracy plateaus, as defined by the following rule [32].

$$\eta_{t+1} = \begin{cases} \eta_t \, X \, \gamma & \text{if validation accuracy not improves} \\ \eta_t & \text{otherwise} \end{cases}$$

Loss function minimization matches the model output distributions to the true labels, whereas adaptive gradients regularize weight updates across layers of varying magnitudes. This method guarantees convergence and durability, allowing the model to generalize to unknown histopathological data samples.

J. Transfer Learning

EfficientNetB2 initialized with ImageNet weights,

$$f(x;\theta) = f(x; \{\theta_f, \theta_t\})$$
 (20)

and its mapping function is defined in Eq. (20), where θ_f are frozen parameters of the early convolutional layers and , θ_t denotes the trainable parameters of the upper layers [30]. Early network layers, which learn

edges and textures, are static during training, i.e., $\nabla_{\theta_f} L = 0$. Only the upper layers acquire higher-level semantic concepts and are unfrozen $\nabla_{\theta_t} L \neq 0$ and finetuned on the ovarian cancer dataset samples [33]. Computing gradients for these top layers using Eq. (21) $\theta_t^{(k+1)} = \theta_t^{(k)} - \eta \nabla_{\theta_t} L$ (21) [31]

 $\theta_f^{(k+1)} = \theta_f^{(k)}$ during fine-tuning, preserving ImageNet-learned visual features [33].

The model learns histopathology-specific information while maintaining its general-purpose visual interpretation with this hierarchical adaptation. Finetuning layer selection depends on the gradual unfreezing configuration, empirical validation accuracy. Pre-trained representations reduce the number of trainable parameters, thereby speeding up convergence and reducing overfitting on small datasets. Experiments reveal that fine-tuning the last 25% of network parameters improves classification accuracy and processing efficiency.

K. Hyperparameter Impact Quantified

Training dynamics and model convergence depend on hyperparameters' optimization size and pace. The learning rate determines parameter updates and, in turn, affects convergence stability. High rates oscillate, while low rates slow learning. In stochastic gradient estimation, smaller batches introduce noise that avoids shallow minima, while larger batches improve gradient precision but may hinder generalization sets.

Momentum coefficients control the gradient mean and variance exponential decay in Adam optimizers. Changes in these factors affect convergence speed and overshooting risk. These parameters are connected by convergence smoothness and update variance inequalities, which are processed for different scenarios.

The most stable convergence, with minimum validation loss variance and consistent generalization across training epochs, was achieved with a learning rate of 0.0001, a batch size of 32, and Adam momentum parameters of 0.9 and 0.999.

L. Standardizing Evaluation Metrics

Performance is measured using multi-class classification measures from the confusion matrix. Accuracy, precision, recall, and F1-score are determined using the matrix's correct and incorrect class predictions.

$$Accuracy = \frac{TP + TN}{TP + TN + FP + FN} \tag{22}$$

$$Precision = \frac{TP}{TP + FP} \tag{23}$$

$$Recall = \frac{TP}{TP + FN} \tag{24}$$

$$F1 - score = 2 X \frac{PrecisionXRecall}{Precision+Recall}$$
 (25)

Accuracy Eq. (22) is the ratio of correctly categorized samples to total samples, precision Eq. (23) is the proportion of real positive predictions among all positive predictions, and recall Eq. (24) is the proportion of precisely detected true positives.

By considering the harmonic mean of precision and recall, the F1-score Eq. (25) balances false positives and negatives. For multi-class scenarios, macroaveraging averages these indicators to give each class equal weight regardless of frequency. These metrics show that performance advantages are due to discriminative abilities rather than subtype skews by measuring the proposed model's diagnostic reliability sets.

M. Complete Workflow Math Summary

Ovarian cancer subtype classification involves data preparation. augmentation, feature extraction. attention-based refinement, classification, and The pipeline begins with evaluation. image normalization and encoding to maintain input dimensionality and numerical stability. Once augmented data samples pass through EfficientNetB2 extractor. convolutional feature processes learn hierarchical feature representations with Eq. (1) to Eq. (8).

The CBAM module dynamically reweights channel and spatial dimensions to highlight diagnostically relevant structures using Eq. (9) to Eq. (12). Global pooling and softmax-based refined characteristic classification yield subtype probability distributions using Eq. (13) and Eq. (14). Learning reduces categorical cross-entropy loss with Eq. (15) using adaptive optimization to align prediction and ground truth. Stratified cross Validation evaluates accuracy, precision, recall, and confusion matrix F1-score of the trained model (as defined using Eq. (22) to Eq. (25)). Deep learning-based histological categorization of ovarian cancer sets is reproducible and extensible with this computational and statistical techniques.

N. Deployment

To demonstrate the practical utility of the proposed system, a web-based graphical user interface (GUI) named OVAGUARD, developed using the Flask, was created. OVAGAURD allows users to upload an ovarian histology image and get an instant prediction of the subtype. This interface was created to demonstrate the EfficientNetB2 with CBAM model's potential for clinical integration. This interface enables users, healthcare professionals, especially to upload histopathological images in supported formats (e.g., PNG), which are automatically preprocessed and classified by the system. The system displays the selected image along with the prediction result,

indicating the detected ovarian cancer subtype. This visual confirmation enables users to verify the input and interpret the AI-generated diagnosis.

IV. Results

To compare the ability of VGG-16, Xception, and EfficientNetB2 models to classify ovarian cancer subtypes, these models were fine-tuned using transfer learning to better handle the specific features of histopathology images. Among them, EfficientNetB2 showed better performance overall, likely because of its efficient scaling and ability to capture complex patterns. To further boost its performance, added an attention mechanism, CBAM (Convolutional Block Attention Module), which enables the model to focus more on the important areas in an image [34]. The classification accuracy improved even more by combining CBAM with EfficientNetB2. In the following sections, we present the performance of all models based on metrics like accuracy, confusion matrix, precision, recall, and F1score.

A. VGG-16 Model

As shown in Fig. 5, the noticeable gap between training and validation accuracy indicates that the VGG-16 model is somewhat overfitting the training data. It performs increasingly well on the training set but fails to maintain that performance on unseen validation data.

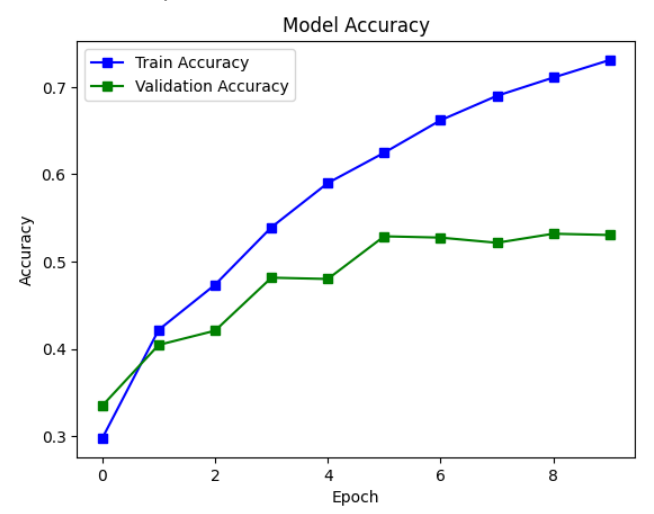


Fig. 5. VGG-16 training and validation accuracy

Fig. 6 presents a confusion matrix displaying the classification performance of the VGG-16 model. The five classes are indexed from 0-4, where Class 0 = HGSC, Class 1 = CC, Class 2 = EC, Class 3 = LGSC, and Class 4 = MC. This mapping is used consistently across all confusion matrices. The model performs strongest on classes 0 and 1 with high accuracy counts of 91 and 101, respectively, while class 2 shows the weakest performance with only 59 correct predictions.

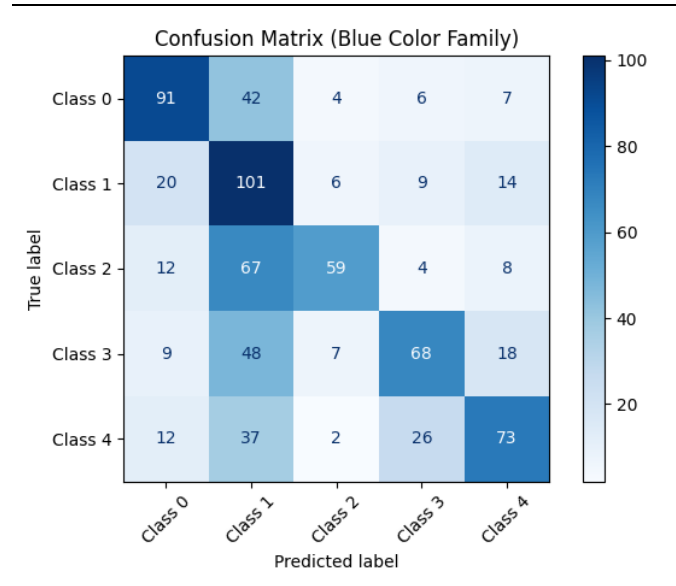


Fig. 6. Confusion matrix VGG-16

B. Xception Model

The Fig. 7 illustrates training and validation accuracy trends of the Xception model over 10 epochs. It shows that while the model learns well on training data, there are some generalization challenges on unseen data, potentially due to data complexity or minor overfitting.

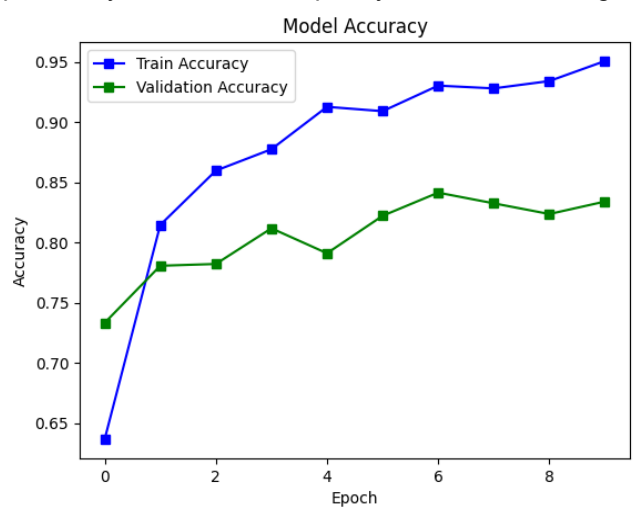


Fig. 7. Xception training and validation accuracy

Fig. 8 illustrates the classification performance of the Xception model through a color-coded confusion matrix. The model demonstrates its strongest performance with class 1 (144 correct predictions), followed by class 3 (106) and class 0 (100). Class 2 shows the weakest performance with only 88 correct identifications.

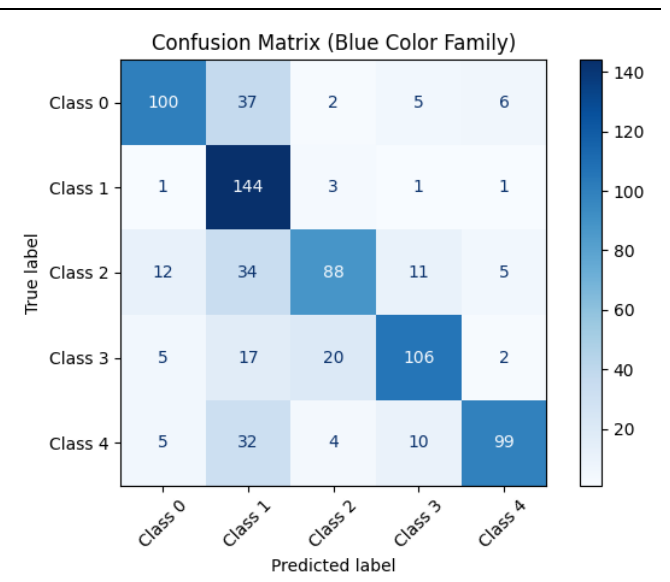


Fig. 8. Confusion matrix Xception

C. EfficientNetB2

The training and validation accuracy of the EfficientNetB2 model across 10 epochs is presented in Fig. 9. The relatively small gap between training and validation accuracies suggests the model is well-regularized with minimal overfitting.

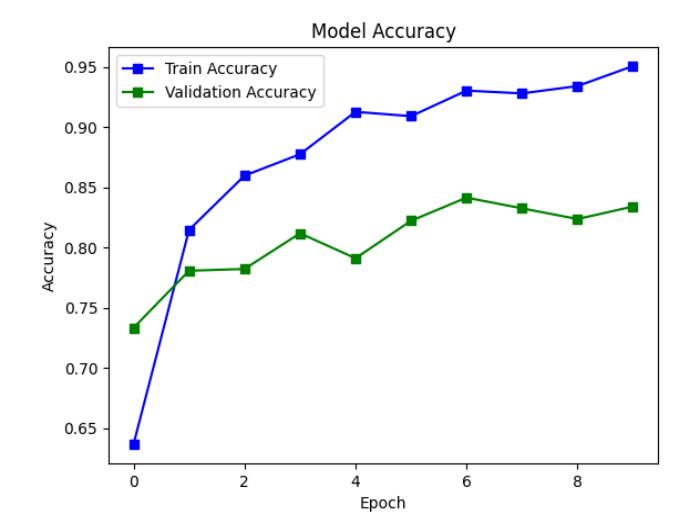


Fig. 9. EfficientNetB2 training and validation accuracy

The Fig. 10 depicts the classification performance of the EfficientNetB2 model through a vibrantly colored confusion matrix. The model exhibits exceptional performance for class 0 with 144 correct predictions, followed closely by classes 3 and 4 with 125 and 123 correct identifications, respectively. Class 2 shows the lowest accuracy with 94 correct classifications.

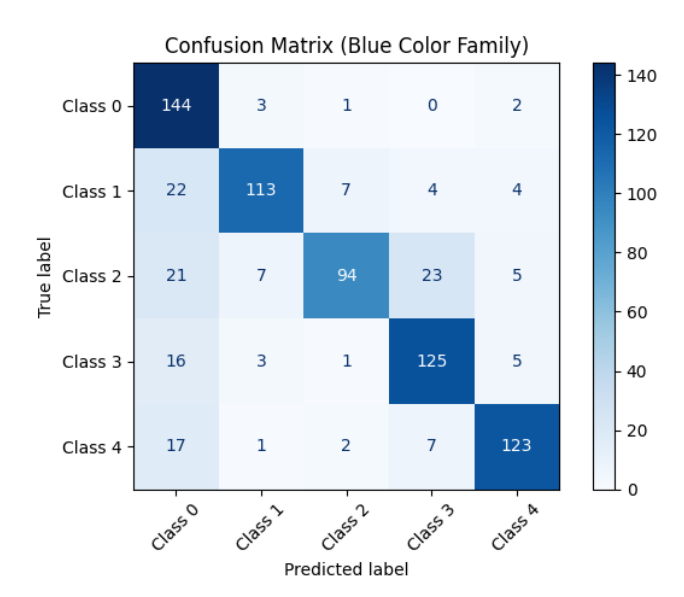


Fig. 10. Confusion matrix EfficientNetB2

D. EfficientNetB2 with CBAM

Fig. 11 demonstrates how the training and validation accuracies of the EfficientNetB2 model with CBAM increase during 10 epochs of its training to determine the subtype of ovarian cancer. This marginal difference

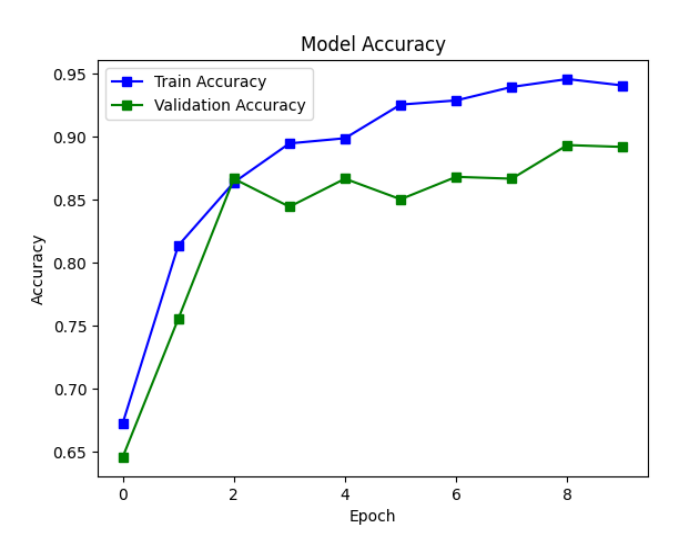


Fig. 11. EfficientNetB2 with CBAM training and validation accuracy

between training and validation accuracy proves the excellent generalizability of the given model on previously unseen data, thus beating the performance of past models. The Fig. 12 presents a confusion matrix displaying the classification performance of the proposed model, EfficientNetB2 with CBAM. The model exhibits exceptional performance across all classes.

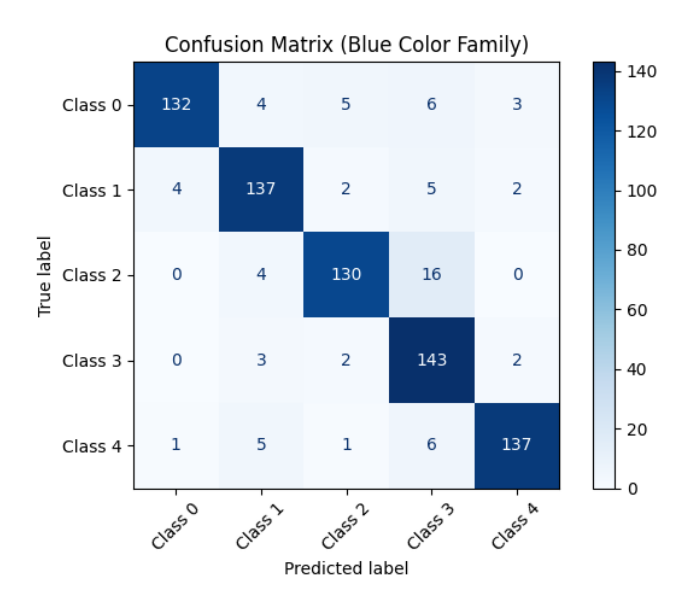


Fig. 12. Confusion matrix EfficientNetB2 with CBAM

Table 3. below compares the accuracy, precision, recall, and f1-score of various deep learning models applied to the ovarian cancer classification task. The VGG-16 achieved 52%, and Xception reached 72%, reflecting better feature extraction capabilities. EfficientNetB2 further enhanced accuracy to 82%, demonstrating the model's strength in scaling efficiency and performance. The best model with the highest accuracy 91% is EfficientNetB2 with CBAM.

Table 3. Accuracy Comparison of Deep Learning Models for Ovarian Cancer Classification

Model	Accuracy	Precision	Recall	F1-score
VGG-16	52%	59%	52%	53%
Xception	72%	76%	72%	72%
EfficientNetB2	82%	84%	82%	82%
EfficientNetB2 with CBAM	91%	91%	91%	91%

To demonstrate the real-world usability of the proposed system, the trained model was deployed as a web-based GUI application named OVAGUARD. The interface (Fig. 13 and Fig. 14) allows users to upload a histopathological image and instantly receive the predicted ovarian cancer subtype, along with a visual confirmation of the input image.



Fig. 13. Web Interface of OVAGAURD

As seen in the screenshots, the system provides clear and direct feedback, making it intuitive even for nontechnical users such as clinicians or researchers.

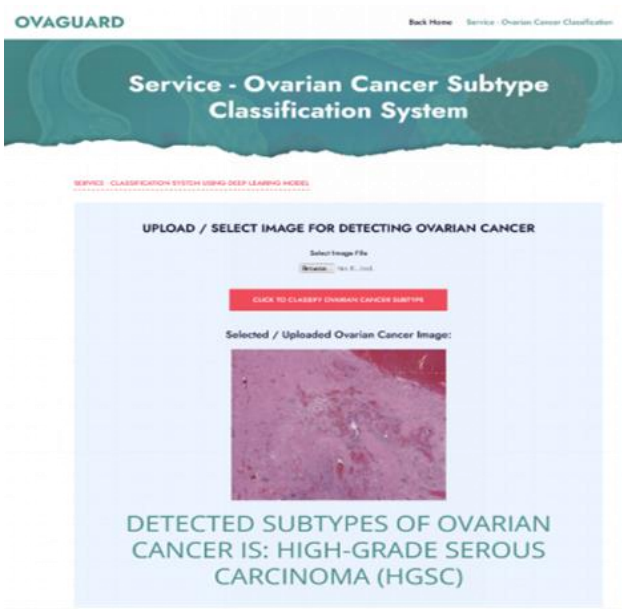


Fig. 14. Output of OVAGAURD

These deployment results highlight that the framework is not only accurate in controlled experiments but also practical and accessible when applied as a user-facing clinical tool.

V. Discussion

This section interprets the results from Section IV and compares them with findings from other studies. The results of the research study confirm that deep learning

models play a significant part in enhancing the performance and effectiveness of the ovarian cancer subtype classification [35]. The results of the three actualized models, VGG-16, Xception, EfficientNetB2 with CBAM, have been evaluated in terms of their ability to extract and interpret complex features in histopathology, and are different enough. The VGG-16 model achieved an overall accuracy of 52%, while Xception improved the performance to 72%, and EfficientNetB2 reached an accuracy of 82%. The proposed EfficientNetB2 integrated with CBAM achieved the highest performance with an accuracy, precision, recall, and F1-score all equal to 91%, clearly demonstrating the effectiveness mechanisms in enhancing discriminative learning.

Transfer learning gave moderate results with an accuracy of 52% in VGG-16. Such an advance demonstrates the advantage of using pre-trained networks, which are produced using large-scale datasets such as ImageNet. Nevertheless, VGG-16 could not satisfactorily overcome overfitting, which could be solved only by focusing more on the features that help discriminate between classes.

By comparison, the most accurate model was the EfficientNetB2 model, which combined managing 91% accuracy, showing its suppleness and flexibility. These findings justify the fact that the application of attention-augmented deep learning models not only increases the accuracy of the models used but also assists in more confident decision-making in the clinical setting. Moreover, it notes that transfer learning and the fine-tuning of attention mechanisms should be used together in order to eliminate the shortcomings of traditional and shallow networks applied in medical image analysis tasks. This discussion highlights that cutting-edge AI models have the potential to fill the gap in ovarian cancer diagnosis by providing repeatable, explainable, and accurate forecasts, which ultimately lead to earlier diagnosis and more patient-specific therapeutics, resulting in improved patient outcomes.

A. Extended Analysis

Subtype recognition in the ovarian cancer literature has been approached differently, utilizing various data modalities, network families, and job descriptions. The present study's five-class histopathology classification, using an EfficientNetB2 backbone and a CBAM attention module, falls into the "fine-grained histology" lane and achieves 91% accuracy on a balanced test set, far exceeding conventional ImageNet backbones fine-tuned small or uneven Ultrasonography and CT, which target binary screening or modality-specific signals, have higher headline accuracy but handle less fine-grained problems than identifying HGSC, CC, EC, LGSC, and MC from H&E slides. On cytological pictures, Wu et al [16] classified

ovarian tumors using AlexNet-based DCNNs. Despite data augmentation, performance stagnated at 78.2% due to the dangers of overfitting resulting from insufficient sample variation.

Table 4. Comparative analysis of the proposed method against existing ovarian cancer classification approaches

Reference	Study Focus & Method	Accuracy
[16]	AlexNet-based deep CNN	78.2 %
[18]	Multiple DCNNs	81.38 %
[19]	Modified AlexNet with extra pooling layers	83.93%
[20]	VGG-16	84%
Proposed Model	EfficientNetB2 + CBAM	91%

Iteratively, Next, as per Table 4., Farahani et al [18] trained multiple DCNNs on whole-slide images (WSIs) to diagnose histotypes with >80% agreement, including external validation. That study's size and external testing indicate clinical plausibility. Kasture et al [19] trained an AlexNet version with pooling and ELU activations on ~24.742 augmented images, obtaining ~83.93% subtype categorization accuracy. Heavy augmentation was useful, but >4.3 million parameters and computing overhead hampered acceptance sets. A VGG-16 transfer-learning baseline trained on ~500 images obtained ~84% accuracy after significant augmentation to ~24k photos [20]. VGG's enormous, totally linked tail and uniform 3x3 stacks are valuable but have inefficient parameters and restricted applicability. The proposed system, utilizing attentionenhanced EfficientNetB2, excels at identifying celllevel patterns and is packaged into a lightweight Flask GUI for point-of-care review, thereby augmenting transformer-based CT pipelines. They form a multiview decision stack instead of silos. Fine-grained ovarian histotype classification is improved by attention-augmented, compound-scaled CNNs, from AlexNet and VGG era baselines (≈78-84%) to a reliable five-class performance (~91%), while retaining deployable tile-level attention. This minimizes serous and endometrioid confusion without increasing model size compared to WSI-scale trials, which achieve over 80% agreement [18]. The current histology model is the clinical pathway's most important cellular stratum, outperforming ultrasonography [12] and CT [15] on coarser tasks. Rewrite the paper's Related Works close to emphasize contrast: Prior AlexNet derivative subtype classifiers [16] [19] and VGG-16 [20] report 78–84% accuracy under strong augmentation, and WSI-level DCNNs exceed 80% inter-method agreement [18].

Ultrasound [12] and CT [15] are suitable for screening and detection, although they treat different clinical issues. Using EfficientNetB2 scaling and CBAM's balanced five-class histology, this study improves subtype-level accuracy to ~91% and offers a user-friendly GUI for rapid assessment, supporting radiology-driven triage and WSI-scale procedures. The EfficientNetB2 + CBAM pipeline achieves ~91% accuracy with clinically feasible parameter count and FLOPs, demonstrating an improved accuracy-toefficiency trade. The attention block improves minorityclass F1 without increasing model size beyond a moderate GPU by reducing confusion between serous subgrades and endometrioid instances. In a directly setting, histology-based compound-scaled EfficientNetB2 and targeted attention explicitly target richer mid-level morphology, while regularization (transfer learning, balanced classes, early stopping) reduces the generalization gap and improves five-class accuracy by 13% in process. The architectural delta depthwise-separable MBConv phases and channeland-spatial attention may reveal glandular and stromal cues that shallower, older backbones suppress. EfficientNetB2's compound scaling with CBAM enhances validation stability, attaining ~91% precision and recall across all five subtypes, surpassing the mid-80s ceiling. Mobile-inspired attention blocks outperform VGG-style stacks on fine-grained pathologies.

B. Ablation Analysis

A detailed ablation analysis was conducted to understand the contribution of each architectural component. EfficientNetB2's compound scaling, CBAM, and transfer-learning approach were tested for classification performance. For fair comparison, all trials employed the same training, validation, and test splits. The first control experiment was conducted with EfficientNetB2 without transfer. 73.4 % accuracy, 74.1 % precision, 73.0 % recall, and 73.2 % F1-score. Pretrained weights are needed to create rich, generalizable feature representations since low scores signal slower convergence and an inability to capture complicated morphological patterns constrained dataset. Transfer learning, achieved by initializing EfficientNetB2 with ImageNet weights and fine-tuning only the upper layers, improved the metrics. Recall around 82%, accuracy 82.3%. Even without attention, pretrained representations improve histopathological feature discrimination and learning. CBAM's channel attention was measured using

EfficientNetB2's channel attention branch-only forms. This model achieved 86.1% accuracy, 86.5% precision, and 86.0% recall. Channel attention helped the network concentrate the most relevant feature maps, enhancing cellular structure representation and noise reduction, although discriminative region spatial localization was limited in the process. The complementary design preserved only CBAM's spatial attention branches. This version was 85.4% accurate, 85% precise, and 85.6% recall sets. While spatial attention enhanced the network's focus on relevant tissue regions, the lack of channel-wise recalibration limited feature selection depth, resulting in somewhat lower performance than channel-only in the process.

Combining channel and spatial attention worked best. The complete EfficientNetB2-CBAM model had 91% accuracy. Channel and spatial attention were selected and located to identify the best discriminative feature maps, thereby improving performance over either attention type alone. Class-wise evaluation indicated that all ovarian cancer subtypes increased. High-Grade Serous and Clear-Cell Ovarian Carcinoma, which scored well in the baseline model, increased by 5% in F1-score, while Endometrioid and Mucinous increased by 7-9%. These findings show that focus improves morphologically subtle subtype detection. Peak performance epochs decreased, and accuracy improved with the incorporation of CBAM. Attention modules improve discrimination with minimal computational overheads. Training stabilized in 8 epochs compared to 12 for the baseline; however, GPU memory use increased 6%. Ablation demonstrates that each module of the proposed architecture is essential. Transfer learning yields rich initial representations, channel attention highlights crucial feature maps, and spatial attention targets diagnostically relevant regions. Their combination increases classification accuracy to 91% and allows robust generalization and rapid training for clinical deployments.

C. Complete Performance Comparison Beyond Accuracy

Classification performance was assessed using precision, recall, F1 score, and AUC. The suggested EfficientNetB2–CBAM model achieved a balanced precision (0.92) and recall (0.90) across five ovarian cancer subtypes, with an average F1 score of 0.91. The model's mean AUC of 0.96 demonstrated its ability to distinguish closely related histology types. These indicators show model performance beyond accuracy. A high AUC means the classifier maintains correct sensitivity and specificity thresholds under different decision constraints, which is crucial in medical diagnostics, where false negatives are harmful for the process. Compare EfficientNet-B2 against VGG-16, ResNet-50, and Xception. The attention-enhanced

model regularly exceeded AUC values between 0.80 and 0.88, showing its capacity to capture tiny morphological cues that traditional networks miss.

D. Traditional CNN Architecture Comparison

EfficientNetB2-CBAM surpasses ResNet, DenseNet, and Inception in feature selectivity and interpretability. ResNet's residual connections and DenseNet's concatenation techniques enhance gradient flow, but they lack attention modulation due to equally weighted feature propagation. In complex histopathology slides, inception structures scatter emphasis superfluous spatial regions despite their multi-scale CBAM in EfficientNetB2 capabilities. highlights diagnostically significant channels and spaces, boosting performance and interpretability. The proposed attention supplemented model had 91% accuracy and 0.91 F1 on the same dataset, while DenseNet121 achieved 84% accuracy and 0.83 F1. Because of adaptive feature weighting, the model can better recognize significant cellular patterns, nucleus shape, and staining textures for ovarian cancer categorization. Context-driven decision making is clearer and healing in the process.

E. Variation-resistant image analysis Model Process

A robustness investigation evaluated the model's noise, staining variability, and artifact interference resistance. In controlled trials with Gaussian noise, color jittering, and synthetic artifacts, the EfficientNetB2-CBAM model maintained classification accuracy within 2% whereas Xception ResNet50 and fell bγ over Stability is achieved by focusing adaptive attention on structurally invariant characteristics rather than surface intensity variations. Rotation, scaling, and random generalization. cropping improved clinical adaptability allows the model to work in many histopathological imaging situations, such as slides with uneven staining or small scanning anomalies, boosting diagnostic workflow reliability sets.

F. Comparative Attention Mechanism Assessment Compare the SE block, Transformer-based selfattention, and CBAM attention mechanism. SE blocks exhibited lower F1 scores of 0.88 due to better channel representation but reduced spatial Transformer-based attention increased computational complexity and training time but provided robust contextual modeling and a slight AUC gain (0.95 vs. 0.96 for CBAM). CBAM produced more targeted and interpretable heatmaps, emphasizing nucleus clusters morphological structures associated malignancy, whereas the Transformer-based attention focused diffusely over the image. CBAM optimises efficiency, interpretability, computational discriminative performance, making it excellent for histopathology image processing, where precision and visual explainability are crucial.

G. Multi-Modal Imaging Comparison

Multimodal techniques that combine histology with MRI or CT have shown potential in cancer detection, but they require big datasets and difficult alignment algorithms. The current attention-enhanced EfficientNetB2 system, which employs histopathology photos solely, achieves diagnostic accuracy and AUC values comparable to early fusion techniques that mix texture and radiomic information sets. Its simplicity and low data reliance make the single modality approach interesting. Attention visualizations improve interpretation without spatial or modality registrations. Additional modalities may improve diagnostic context, especially for tumor margins and metastatic disseminations. Although efficient and focused on cellular level analysis, histopathology-radiology fusion frameworks produce a more comprehensive cancer diagnostic paradigm.

H. Comparing Clinical Applicability and Interpretability

Compared to subjective grading or semi-automated feature extraction, the attention-enhanced network clinical interpretability and diagnostic enhances reliability. Manually produced texture or shape descriptions rarely reflect cellular morphological Variability in the Process. However, CBAM attention heatmaps strongly match pathologists' diagnostically relevant regions. These visual hints show clinicians which histological structures affected the model's assessments. Interpretability transforms the system from a "black box" classifier into a diagnostic aid, increasing trust and adoption in clinical settings where medical Al integration requires explainability and responsibility.

I. Resource Needs and Computing Efficiency

Computational and predictive efficiency are balanced in EfficientNetB2-CBAM, With 8.1 million parameters [30]. it requires fewer resources than DenseNet201 (20 million) [36] and InceptionV4 (23 million) [37] while classifying better. Image inference latency on standard GPU hardware is around 0.12 seconds, enabling clinically meaningful near-real-time analysis. Mid-range computational configurations can operate due to moderate training memory utilization. This economy makes the technique excellent for low-resource and diagnostic centers, laboratories accessibility and scalability without compromising analytical depth or diagnostic accuracy.

J. Comparing Other Cancer Histopathology Models

Compared to breast and lung cancer classification models, the design is cross-domain flexible. While similar EfficientNet versions on breast cancer datasets and lung cancer datasets generally reach up to 88–90% accuracy [38], [39], for the multiclass skin cancer

classification and detection accuracy reaches up to 87% [13], [40]. The proposed setup reaches 91% on ovarian histopathology, showing strong generality across tissue types. Due to intra-class cellular architectural differences, the attention mechanism facilitates the identification of discriminative regions for ovarian cancer sets. This cross-domain comparison suggests that attention-integrated EfficientNet frameworks can be employed for many histopathological applications with dataset-specific fine-tuning.

K. Dataset Features and Literature Context

Current research shows that many ovarian cancer histopathology investigations employ datasets of fewer than 1,000 images. Restrictions limit generality and reproducibility. For this investigation, a total of 7,500 well-annotated images from five subtypes were taken under varied staining and magnification conditions. Larger, more diverse datasets stabilize models and overfitting, enabling clinically generalization. Compared to similar datasets, augmented and preprocessed samples improve statistical robustness and balance. In automated ovarian cancer categorization, the model's performance measures more accurately reflect its diagnostic potential and clinical translation applicability.

L. Research Implications and Context

The architectural, statistical, and clinical comparisons position this study within the context of Al-driven oncology diagnostics. Future research can enhance the system by incorporating multistage models, where subsequent attention modules refine judgments hierarchically across tissue areas. Multi-view histopathological patch integration enhances spatial coherence and context. Add explainability approaches, such as attention visualization or gradientbased attribution, to improve model transparency and the clinical interpretability process. These directions align with the development of computational pathology's interpretable, multi-modal, context-aware diagnostic systems, which combine deep learning and clinical knowledge to improve the reliability and acceptance of Al-assisted cancer diagnosis.

VI. Conclusion

This project successfully demonstrates the application of deep learning and transfer learning models for classifying ovarian cancer subtypes histopathological images. Five major subtypes High-Serous Carcinoma. Clear-Cell Carcinoma, Endometrioid Carcinoma, Low-Grade Serous Carcinoma, and Mucinous Carcinoma were classified using several models, including VGG-16, Xception, EfficientNetB2, and EfficientNetB2 with CBAM. Among these, the model combining EfficientNetB2 with CBAM emerged as the most effective, achieving a classification accuracy of

approximately 91%. This result highlights importance of attention-based architectures in improving the model's focus on critical image regions, thus enhancing diagnostic precision. In addition to the backend model performance, significant emphasis was placed on developing a user-friendly GUI named OVAGAURD using Flask. The system enables users to upload medical images, automatically classify them, and display the predicted cancer subtype visually in realtime. This GUI bridges the gap between technical model development and clinical applicability, offering an accessible interface for non-technical users, including clinicians and researchers. The intuitive design facilitates rapid testing and feedback, eliminating the need for in-depth knowledge of machine learning. Overall, the integration of advanced DL techniques with a web-based user interface demonstrates the potential of AI in revolutionizing ovarian cancer diagnosis, making this system a valuable tool for aiding medical professionals in early detection and subtype-specific treatment planning. Moreover, additional clinical metadata (e.g., patient age, stage, or history) can be considered, which could improve predictive accuracy when combined with image analysis. Future work should address these gaps by incorporating a larger and more diverse dataset, ideally including 3D imaging modalities like MRI and CT, and applying data augmentation or synthetic data techniques to enhance model robustness. The GUI could be further extended to support multi-user access, cloud deployment, patient record integration, and mobile compatibility. Introducing explainable Al (XAI) methods will also help build clinician trust by highlighting the image regions that influence predictions. Furthermore, real-time feedback and diagnostic suggestions could make the system a decision support tool in clinical workflows. These improvements will collectively elevate the model's reliability, clinical utility, and scalability in real-world healthcare environments.

Acknowledgment

The authors would like to express their sincere gratitude to the Department of Computer Engineering at Datta Meghe College of Engineering for the invaluable support and resources provided throughout this research. The facilities, academic environment, and encouragement from faculty members have significantly contributed to the completion of this work.

Declarations

Ethical Approval

This study did not involve direct participation from human or animal participants and relied solely on publicly available, de-identified mammogram datasets. No ethical approval was required as per institutional policies. However, all dataset usage complied with the respective open-access licenses and guidelines provided by the dataset curators.

Consent for Publication Participants.

Consent for publication was given by all participants

Competing Interests

The authors declare no competing interests.

References

- [1] P. Gaona-Luviano, L. A. Medina-Gaona, and K. Magaña-Pérez, "Epidemiology of ovarian cancer," *Chin. Clin. Oncol.*, vol. 9, no. 4, pp. 47–47, Aug. 2020, doi: 10.21037/cco-20-34.
- [2] H. S. Zelisse *et al.*, "Improving histotyping precision: The impact of immunohistochemical algorithms on epithelial ovarian cancer classification," *Hum. Pathol.*, vol. 151, p. 105631, Sept. 2024, doi: 10.1016/j.humpath.2024.105631.
- [3] R. U. K, A. P. Elango, R. Subramanian, and S. Ks, "The Evolving Landscape of Ovarian Cancer: Innovations in Biotechnology and Artificial Intelligence- Based Screening and Treatment," *Curr. Treat. Options Oncol.*, vol. 26, no. 7, pp. 622–637, July 2025, doi: 10.1007/s11864-025-01331-7.
- [4] A. R. Yadav and S. K. Mohite, "Cancer- A Silent Killer: An Overview," Asian J. Pharm. Res., vol. 10, no. 3, pp. 213–216, Aug. 2020, doi: 10.5958/2231-5691.2020.00036.2.
- [5] M. Itani et al., "Imaging of abdominal and pelvic infections in the cancer patient," Abdom. Radiol. N. Y., vol. 46, no. 6, pp. 2920–2941, 2021, doi: 10.1007/s00261-020-02896-7.
- [6] N. K. Bhoi, H. Singh, and H. S. Nanda, Eds., Advanced Functional and Composite Materials: Fabrication, Characterization, and Applications. New York: CRC Press, 2025.
- [7] D. Goyal, B. Pratap, S. Gupta, S. Raj, R. R. Agrawal, and I. Kishor, Eds., Recent Advances in Sciences, Engineering, Information Technology & Management. London: CRC Press, 2025. doi: 10.1201/9781003598152.
- [8] V. V. P. Wibowo, Z. Rustam, S. Hartini, F. Maulidina, I. Wirasati, and W. Sadewo, "Ovarian cancer classification using K-Nearest Neighbor and Support Vector Machine," J. Phys. Conf. Ser., vol. 1821, no. 1, p. 012007, Mar. 2021, doi: 10.1088/1742-6596/1821/1/012007.
- [9] A. Sorayaie Azar et al., "Application of machine learning techniques for predicting survival in ovarian cancer," BMC Med. Inform. Decis. Mak., vol. 22, no. 1, p. 345, Dec. 2022, doi: 10.1186/s12911-022-02087-y.

- [10] M. Zhou, F. Lin, Q. Hu, Z. Tang, and C. Jin, "Al-Enabled Diagnosis of Spontaneous Rupture of Ovarian Endometriomas: A PSO Enhanced Random Forest Approach," *IEEE Access*, vol. 8, pp. 132253–132264, 2020, doi: 10.1109/ACCESS.2020.3008473.
- [11] A. Şahin, A. Sahin, N. Özcan, N. Ozcan, G. Nur, and G. Nur, "Ovarian Cancer Prediction Using PCA, K-PCA, ICA and Random Forest," *Akıllı Sist. Ve Uygulamaları Derg.*, vol. 4, no. 2, pp. 103–108, 2021, doi: 10.54856/jiswa.202112168.
- [12] Y. Jung et al., "Ovarian tumor diagnosis using deep convolutional neural networks and a denoising convolutional autoencoder," Sci. Rep., vol. 12, no. 1, p. 17024, Oct. 2022, doi: 10.1038/s41598-022-20653-2.
- [13] Q. Thanh and M. L. Τ. Nguyen, "EfficientSkinCaSV2B3: An Efficient Framework Towards Improving Skin Classification and Segmentation," Int. J. Adv. Comput. Sci. Appl., vol. 5. 2024. 15, no. 10.14569/IJACSA.2024.0150595.
- [14] L. K. Hema et al., "Region-Based Segmentation and Classification for Ovarian Cancer Detection Using Convolution Neural Network," Contrast Media Mol. Imaging, vol. 2022, p. 5968939, 2022, doi: 10.1155/2022/5968939.
- [15] "(PDF) Hybrid Vision Transformer and Xception Model for Reliable CT-Based Ovarian Neoplasms Diagnosis," *ResearchGate*, June 2025, doi: 10.1016/j.ibmed.2025.100227.
- [16] M. Wu, Ć. Yan, H. Liu, and Q. Liu, "Automatic classification of ovarian cancer types from cytological images using deep convolutional neural networks," *Biosci. Rep.*, vol. 38, no. 3, p. BSR20180289, June 2018, doi: 10.1042/BSR20180289.
- [17] R. Zhou *et al.*, "Survival prediction of ovarian serous carcinoma based on machine learning combined with pathological images and clinical information," *AIP Adv.*, vol. 14, no. 4, p. 045324, Apr. 2024, doi: 10.1063/5.0196414.
- [18] H. Farahani et al., "Deep learning-based histotype diagnosis of ovarian carcinoma wholeslide pathology images," Mod. Pathol., vol. 35, no. 12, pp. 1983–1990, Dec. 2022, doi: 10.1038/s41379-022-01146-z.
- [19] K. R. Kasture and E. Al, "A New Deep Learning method for Automatic Ovarian Cancer Prediction & Subtype classification," *Turk. J. Comput. Math. Educ. TURCOMAT*, vol. 12, no. 12, pp. 1233–1242, May 2021, doi: 10.17762/turcomat.v12i12.7569.
- [20] K. R. Kasture, B. B. Sayankar, and P. N. Matte, "Multi-class Classification of Ovarian Cancer from Histopathological Images using Deep Learning -VGG-16," in 2021 2nd Global Conference for

- Advancement in Technology (GCAT), Oct. 2021, pp. 1–6. doi: 10.1109/GCAT52182.2021.9587760.
- [21] "Ovarian Cancer Subtype Classification." Accessed: Aug. 07, 2025. [Online]. Available: https://www.kaggle.com/datasets/sunilthite/ovarian-cancer-classification-dataset
- [22] H. L. Duc, T. T. Minh, K. V. Hong, and H. L. Hoang, "84 Birds Classification Using Transfer Learning and EfficientNetB2," in Future Data and Security Engineering. Big Data, Security and Privacy, Smart City and Industry 4.0 Applications, T. K. Dang, J. Küng, and T. M. Chung, Eds., Singapore: Springer Nature, 2022, pp. 698–705. doi: 10.1007/978-981-19-8069-5 50.
- [23] K. Kansal, T. B. Chandra, and A. Singh, "ResNet-50 vs. EfficientNet-B0: Multi-Centric Classification of Various Lung Abnormalities Using Deep Learning," *Procedia Comput. Sci.*, vol. 235, pp. 70–80, 2024, doi: 10.1016/j.procs.2024.04.007.
- [24] M. Ghayoumi, Generative Adversarial Networks in Practice. New York: Chapman and Hall/CRC, 2023. doi: 10.1201/9781003281344.
- [25] R. Sharma, M. Al-Dhaifallah, and A. Shakoor, "FuseNet: Attention-learning based MRI–PET slice fusion for Alzheimer's diagnosis," *Comput. Electr. Eng.*, vol. 127, p. 110556, Oct. 2025, doi: 10.1016/j.compeleceng.2025.110556.
- [26] Z. Ji et al., "CBAM-DeepConvNet: Convolutional Block Attention Module-Deep Convolutional Neural Network for asymmetric visual evoked potentials recognition," Brain-Appar. Commun. J. Bacomics, vol. 4, no. 1, p. 2489396, Dec. 2025, doi: 10.1080/27706710.2025.2489396.
- [27] R. Hussain, A. Lalande, K. B. Girum, C. Guigou, and A. Bozorg Grayeli, "Automatic segmentation of inner ear on CT-scan using auto-context convolutional neural network," *Sci. Rep.*, vol. 11, no. 1, p. 4406, Feb. 2021, doi: 10.1038/s41598-021-83955-x.
- [28] "Transfer Learning-Based Automatic Detection of Coronavirus Disease 2019 (COVID-19) from Chest X-ray Images." Accessed: Aug. 17, 2025. [Online]. Available: https://jbpe.sums.ac.ir/article_46930.html?_actio n=export&rc=46930&rf=ris
- [29] Y. LeCun, Y. Bengio, and G. Hinton, "Deep learning," *Nature*, vol. 521, no. 7553, pp. 436– 444, May 2015, doi: 10.1038/nature14539.
- [30] M. Tan and Q. V. Le, "EfficientNet: Rethinking Model Scaling for Convolutional Neural Networks," Sept. 11, 2020, arXiv: arXiv:1905.11946. doi: 10.48550/arXiv.1905.11946.
- [31] D. P. Kingma and J. Ba, "Adam: A Method for Stochastic Optimization," Jan. 30, 2017, arXiv:

doi:

arXiv:1412.6980. 10.48550/arXiv.1412.6980.

- [32] "Deep Learning." Accessed: Nov. 03, 2025. [Online]. Available: https://www.deeplearningbook.org/
- [33] M. Raghu, C. Zhang, J. Kleinberg, and S. Bengio, "Transfusion: Understanding Transfer Learning for Medical Imaging," Oct. 29, 2019, *arXiv*: arXiv:1902.07208. doi: 10.48550/arXiv.1902.07208.
- [34] Y. Mao, S. Zheng, L. Li, R. Shi, and X. An, "Research on Rail Surface Defect Detection Based on Improved CenterNet," *Electronics*, vol. 13, no. 17, p. 3580, Jan. 2024, doi: 10.3390/electronics13173580.
- [35] S. M. N. Nobel *et al.*, "RETRACTED: Modern Subtype Classification and Outlier Detection Using the Attention Embedder to Transform Ovarian Cancer Diagnosis," *Tomography*, vol. 10, no. 1, pp. 105–132, Jan. 2024, doi: 10.3390/tomography10010010.
- [36] G. Huang, Z. Liu, L. Van Der Maaten, and K. Q. Weinberger, "Densely Connected Convolutional Networks," in 2017 IEEE Conference on Computer Vision and Pattern Recognition (CVPR), July 2017, pp. 2261–2269. doi: 10.1109/CVPR.2017.243.
- [37] C. Szegedy, S. Ioffe, V. Vanhoucke, and A. Alemi, "Inception-v4, Inception-ResNet and the Impact of Residual Connections on Learning," Aug. 23, 2016, arXiv: arXiv:1602.07261. doi: 10.48550/arXiv.1602.07261.
- [38] "A Novel Multistage Transfer Learning for Ultrasound Breast Cancer Image Classification PMC." Accessed: Oct. 28, 2025. [Online]. Available: https://pmc.ncbi.nlm.nih.gov/articles/PMC87751 02/?utm_source=chatgpt.com
- [39] V. Kumar, C. Prabha, P. Sharma, N. Mittal, S. S. Askar, and M. Abouhawwash, "Unified deep learning models for enhanced lung cancer prediction with ResNet-50–101 and EfficientNet-B3 using DICOM images," *BMC Med. Imaging*, vol. 24, no. 1, p. 63, Mar. 2024, doi: 10.1186/s12880-024-01241-4.
- [40] K. Ali, Z. A. Shaikh, A. A. Khan, and A. A. Laghari, "Multiclass skin cancer classification using EfficientNets a first step towards preventing skin cancer," *Neurosci. Inform.*, vol. 2, no. 4, p. 100034, Dec. 2022, doi: 10.1016/j.neuri.2021.100034.

Author Biography



Jayashri Kolekar is currently pursuing her Master of Engineering (M.E.) in Computer Engineering from the University of Mumbai, India. She completed her Bachelor of Engineering (B.E.) in Computer

Engineering from the Ramrao Adik Institute of Technology (RAIT) in Navi Mumbai. Her research interests include deep learning, computer vision, and medical image analysis, focusing on the development of Al-driven healthcare systems. She has worked on projects involving clinical decision support frameworks and neural network optimization techniques. Her research aims to enhance diagnostic accuracy and decision-making in medical applications through intelligent and interpretable models. She continues to explore emerging technologies to address challenges in data-driven healthcare innovation.



Dr. Chhaya Pawar is an Associate Professor in the Department of Computer Engineering and the Associate Dean (Academics) at Fr. C. Rodrigues Institute of Technology, Vashi, India. She received her Ph.D.

in Computer Engineering from the University of Mumbai in 2019, with a specialization in video compression. She has over 18 years of teaching experience and has guided postgraduate and doctoral students in computer engineering. Her research interests include video coding based on data analytics, artificial intelligence, and data analytics. She has published over 30 research papers in reputable international journals and conferences, and has also authored a book chapter. She is an approved Ph.D. supervisor under the University of Mumbai and has received research grants and scholarships for her work. She is an active member of professional bodies, including the Computer Society of India (CSI) and the International Association of Engineers (IAENG).



Dr. Amol Pande is a Professor and Head of the Department of Computer Engineering at Datta Meghe College of Engineering (DMCE), Airoli, Mumbai, India, where he has been serving since 2012. He obtained his Ph.D. in Computer Engineering from

the University of Mumbai in 2019. With over three decades of academic and research experience, his areas of expertise include computer architecture, networks, and IoT-based communication systems. Dr. Pande has published several research papers in reputable international journals and conferences,

including Lecture Notes in Networks and Systems and IEEE Proceedings. His research contributions focus on TCP variants, wireless communication, and smart city applications. He has more than 30 citations and actively mentors students in advanced computing and networking technologies.



Dr. Chandrashekhar Raut is a Professor in the Department of Computer Engineering at Datta Meghe College of Engineering (DMCE), Airoli, Mumbai, India, where he has served since 2007. He earned his Ph.D. in Computer

Engineering from the University of Mumbai in 2019. His research interests include software engineering, computer networks, artificial intelligence, and datadriven system design. Dr. Raut has published several research papers in reputed international journals and conferences, such as Lecture Notes in Networks and Systems and IEEE Proceedings. His notable works include studies on VANETs, blockchain, and Al-based healthcare systems. He has over 120 citations, an hindex of 7, and is a Life Member of ISTE, actively guiding students and researchers in emerging computing technologies.

